

Sol-Gel Microencapsulation of Organic Molecules: A Structural and Chemical Insight

Alexandra Fidalgo,^[a] Rosaria Ciriminna,^[b] Laura M. Ilharco,^{*[a]} Marzia Sciortino,^[b, c] and Mario Pagliaro^{*[b]}

Dedicated to Professor Roberto Zingales

Silica and organosilica microparticles doped with organic molecules are innovative functional materials with numerous applications in different industries.^[1] Depending on the active molecule to be entrapped, these materials are prepared using a surfactant-assisted sol-gel process, either in a water-in-oil (W/O)^[2] or in an oil-in-water (O/W)^[3] microemulsion, wherein the polycondensation of alkyl alcoxysilanes is actually taking place. Depending on the reaction parameters, full or core/shell spherical microparticles can be obtained with different degrees of encapsulation of the functional active compounds.

The lipophilic molecule dibenzoyl peroxide (BPO) is an important industrial polymerization catalyst.^[4,5] It also has important pharmacological applications owing to its bactericidal activity, mostly for skin diseases such as acne^[6] or rosacea.^[7] Essential oils such as bergamot oil (BO) are well known for their refreshing, relaxing, analgesic, and cicatrizing properties.^[8,9] To enhance the effectiveness of fragrances for the user, fragrance expression is evolving in new forms and functions.^[10] New encapsulation technologies are increasingly used by industry to encapsulate fragrance molecules and then to dispense scent in open spaces such as working and entertainment environments.^[11]

For both BPO and BO, effective sol-gel encapsulation in silica-based microparticles would help prevent their degradation and loss. Recently, comparing two methods for the microencapsulation of BPO,^[12] we concluded that, for industrial applications, methods capable of stabilizing the emulsion system and thus affording homogeneous microparticles were required as microencapsulation must be accompanied by a good degree of control over particle size and shape.

Two such methods are: 1) the ammonia-catalyzed polycondensation of alcoxysilanes assisted by a templating surfactant, such as cetyltrimethylammonium bromide (CTAB), developed by Avnir and co-workers,^[13] and 2) the one-step polycondensa-

tion of alkylalkoxysilanes, catalyzed by 3-aminopropyltrimethoxysilane (APTMS) without any surfactant, introduced by Xin and co-workers.^[14] Both methods afford micron-sized core/shell porous silica spheres, with Avnir's method being already employed for the production of silica-entrapped sunscreens and drugs.^[1]

Herein, we present diffuse-reflectance infrared Fourier transform (DRIFT) spectroscopy results obtained from core/shell particles; we compare the entrapment of BO and BPO in different silica and organosilica particles, obtained from different O/W microemulsions. Along with the efficiency of the encapsulation process, we evaluate some structural aspects of these materials on a molecular scale that will be relevant to their practical application. Indeed, results point to a number of relevant findings.

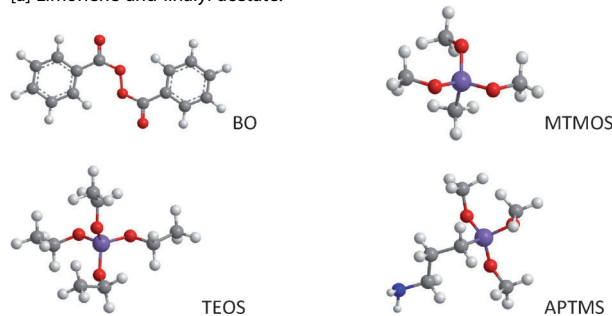
The DRIFT spectra of all the samples listed in Table 1 are shown in Figure 1, and are grouped by silica precursors and translated vertically for better comparison.

All the spectra are typical of condensed silica structures, with bands at 1000–1250 cm⁻¹ (ν_{as} Si-O-Si), approximately 800 cm⁻¹ (ν_s Si-O-Si), and 460 cm⁻¹ (δ Si-O-Si). The presence of uncondensed silanol groups is also visible from the bands at approximately 950 cm⁻¹ (ν Si-OH) and at 3400 cm⁻¹ (ν O-H, mostly related to silanol groups because the water deforma-

Table 1. Labels and composition of the microcapsule samples prepared with different precursors, doped with bergamot oil (BO) or benzoyl peroxide (BPO).

Samples with BO ^[a]	Samples with BPO	Silica precursors	Template + catalyst	Water phase [mL]	Oil phase [mL]	Dopant
MEF8	–	TEOS	CTAB + NH ₄ OH	204	12.2	2 mL
MEF10	–	TEOS	CTAB + NH ₄ OH	204	12.2	2 mL
–	MEB9	TEOS + MTMOS	CTAB + NH ₄ OH	204	13.7	667 mg
MME6	–	MTMOS	APTMS	153	12	3 mL
MME7	–	MTMOS	APTMS	153	12	3 mL
–	MMB4	MTMOS	APTMS	153	12	300 mg

[a] Limonene and linalyl acetate.



[a] A. Fidalgo, Prof. L. M. Ilharco

Centro de Química-Física Molecular and
IN-Institute of Nanoscience and Nanotechnology
Instituto Superior Técnico
Complexo I, Av. Rovisco Pais 1, 1049-001 Lisboa (Portugal)
Fax: (+21) 8464455
E-mail: lilharco@ist.utl.pt

[b] R. Ciriminna, M. Sciortino, Dr. M. Pagliaro
Istituto per lo Studio dei Materiali Nanostrutturati, CNR
via U. La Malfa 153, 90146 Palermo (Italy)
Fax: (+39) 091-680-92-47
E-mail: mario.pagliaro@cnr.it

[c] M. Sciortino
Dipartimento di Ingegneria e Tecnologie Agro Forestali
Università degli Studi, viale delle Scienze 13, 90128 Palermo (Italy)

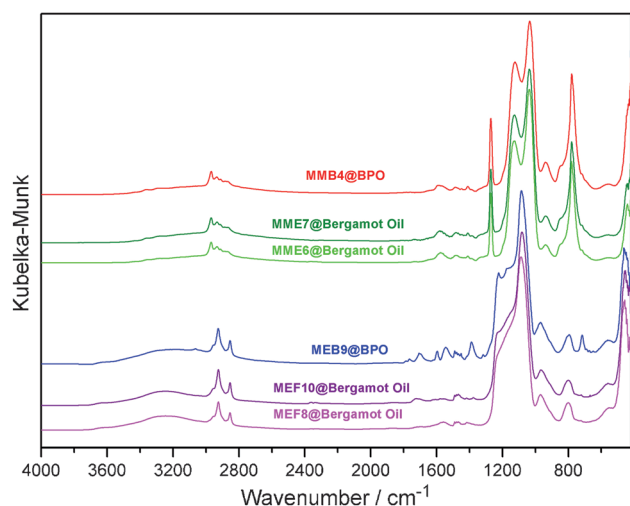


Figure 1. DRIFT spectra of all the microcapsules, normalized to maximum absorption.

tion band is not detected). Generally, the profile of the main silica band (ν_{as} Si-O-Si) clearly changes with the precursors used. The additional bands observed in the spectra are associated with the dopants or additives.

To make a detailed analysis, the more informative spectroscopic regions were enhanced in Figure 2. Figure 2A reveals drastic structural differences between the silica shells, depending on the precursors, evidenced by the ν_{as} Si-O-Si shape and position and by a significant shift in the ν Si-OH band (≈ 30 cm^{-1}): the inorganic samples (**MEF8** and **MEF10**, prepared only from tetraethoxysilane, TEOS, and **MEB9**, prepared from a small proportion of methyltrimethoxysilane, MTMOS) have the ν_{as} Si-O-Si band centered at 1085 cm^{-1} with a high wavenumber shoulder at approximately 1227 cm^{-1} , whereas the organosilica particles (**MME6**, **MME7**, **MEB9**, and **MMB4** prepared from MTMOS) show two resolved bands at approximately 1038 and 1126 cm^{-1} . For MM samples, additional bands appear in this region, at 780 , approximately 850 , and 1271 cm^{-1} , assigned to ρ (Si)CH₃ (superimposing ν_s Si-O-Si), ν Si-C, and δ_s (Si)CH₃ modes, which are characteristic of methylated silica. Other features related with the (Si)-CH₃ groups can be observed in the remaining spectroscopic regions of the MM samples, namely at 1410 cm^{-1} (Figure 2B), 2912 and 2969 cm^{-1} (Figure 2C), assigned to δ_{as} (Si)CH₃, ν_s (Si)CH₃, and ν_{as} (Si)CH₃ modes, respectively. Sample **MEB9** does not present any of these methylsilane groups, which is consistent with a mostly inorganic silica shell.

Bergamot oil is a rich mixture of variable composition, the main components being limonene (1-methyl-4-(1-methylethenyl)-cyclohexene) and linalyl acetate (3,7-dimethyl-1,6-octadien-3-yl acetate), whose spectra have strong C=C stretching bands, at 1644 cm^{-1} , CH₃ and CH₂ stretching and deformation bands, plus a very strong carbonyl stretching corresponding to linalyl acetate.^[15] There are some common features only to **MEF8**, **MEF10**, **MME6**, and **MME7** spectra that are not strong, but are unequivocal fingerprints of this fragrance: the bands at $1717/1700$ (**MEF8**) and $1724/1705$ (**MEF10**), 1737 (**MME6**), and $1740/$

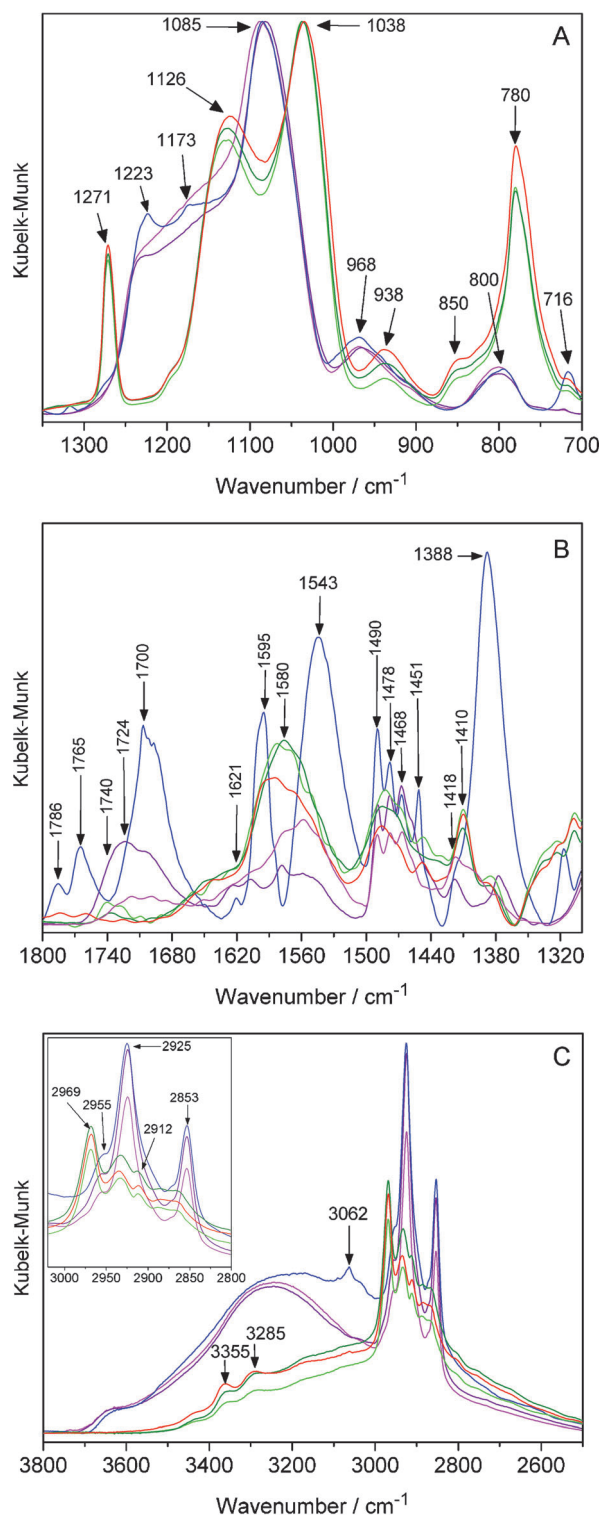


Figure 2. Comparison of the more informative spectroscopic regions, after baseline correction and normalization to the ν_{as} Si-O-Si silica band: **MEF8** (—), **MEF10** (—), **MEB9** (—), **MME6** (—), **MME7** (—), and **MMB4** (—).

1727 (**MME7**), assigned to the ν C=O mode of linalyl acetate, almost unshifted within the hybrid particles and involved in strong hydrogen bonds within the inorganic capsules. The concentration of entrapped bergamot oil in **MEF8** and **MEF10**

is sufficient to detect other typical bands of its more abundant components: $\nu_{as}CH_3$, $\nu_{as}CH_2$, ν_sCH_3 (2955, 2925, and 2853 cm^{-1} , respectively); $\delta_{as}CH_3$, δ_sCH_3 , (1418, 1380 cm^{-1}); $\nu C=C$ in cyclic and acyclic components (a series of bands between 1623 and 1550 cm^{-1}). The positions and relative intensities of these bands indicate that there has been no degradation of the fragrance upon encapsulation or ageing.

The fact that only the carbonyl bands of BO are visible in the **MM** spectra indicates that, although the initial fragrance proportion used in the synthesis was higher, its final content is lower. Thus, the most efficient BO entrapping microcapsules are those prepared by ammonia-catalyzed condensation of tetraethoxysilane (TEOS) assisted by CTAB. The spectra show that BO content increases in the order **MME6** < **MME7** < **MEF8** < **MEF10**. The fresher samples (**MEF10** and **MME7**) show a higher content of fragrance chemicals than the corresponding **MEF8** and **MME6** (prepared six months earlier), thus indicating some loss of fragrance owing to volatilization. Nevertheless, even the oldest and poorer in BO sample (**MME6**) has the characteristic scent of bergamot oil.

The infrared spectrum of BPO is well known,^[16] and even though the O-O stretch originates a very weak infrared band, other fingerprints of the aromatic diacyl peroxide may be identified in the spectrum of sample **MEB9**, at 716 cm^{-1} (out of plane ring deformation), 1173 and 1223 cm^{-1} ($\nu C-O$), 1388 cm^{-1} ($\delta C-H$ in aromatic rings), 1451, 1543, 1595, and 1621 cm^{-1} ($\nu C=C$), 1786/1765 cm^{-1} and approximately 1700 ($\nu C=O$), and 3062 cm^{-1} ($\nu C-H$ in aromatic rings). The fact that the doublets at 1786/1765 cm^{-1} and 1173/1223 cm^{-1} , characteristic of the diacyl peroxide group, are not shifted from their positions in pure BPO indicates that the dopant is not degraded upon encapsulation. The presence of the carbonyl band at approximately 1700 cm^{-1} is a sign that BPO interacts by hydrogen bonding with the silanol groups and the perturbations in the bands related with the aromatic rings indicate that it also interacts with the hydrophobic

groups of the particle shell walls, probably from entrapped surfactant molecules. The sample preparation implied a higher content of BPO in particles **MEB9** than in **MMB4**, and it is confirmed by the DRIFT spectra.

The comparison between the microcapsules containing BO and BPO shows that the silica shells prepared by CTAB-assisted ammonia-catalyzed condensation of TEOS (or TEOS + MTMOS) retain some surfactant, whereas the organosilica shells prepared by polycondensation of MTMOS catalyzed by APTMS retain some catalyst. The presence of APTMS in the three **MM** samples is confirmed by the bands assigned to $\nu_{as}NH_2$, ν_sNH_2 , $\nu_{as}CH_2$, ν_sCH_2 , $\nu_s(Si)CH_2$, δNH_2 , and δ_sCH_3 modes, which appear at approximately 3355, 3285, 2934, 2887, 2867, 1580/1486, and 1388 cm^{-1} , respectively. The presence of CTAB in the three **ME**

Table 2. Band assignments of the DRIFT spectra of the doped inorganic and organosilica microcapsules.

		Wavenumber, $\tilde{\nu}$ [cm^{-1}] ^[a]				Assignment
MEF8@BO	MEF10@BO	MEB9@BPO	MME6@BO	MME7@BO	MMB4@BPO	
3630 _{sh,vw}	3628 _{sh,vw}	3629 _{sh,vw}	3434 _{sh,vw}	3434 _{sh,vw}	3434 _{sh,vw}	$\nu O-H$
			3353 _{sh,vw}	3352 _{sh,vw}	3361 _{sh,vw}	$\nu_{as}NH_2$ (APTMS)
			3284 _{sh,vw}	3286 _{sh,vw}	3285 _{sh,vw}	ν_sNH_2 (APTMS)
3244 _w	3243 _w	$\approx 3200_w$	$\approx 3100_{vw}$	$\approx 3150_{vw}$	$\approx 3160_{vw}$	$\nu O-H$
		3062 _{vw}			3062 _{vw}	$\nu C=H$ (BPO)
			2969 _w	2968 _w	2968 _w	$\nu_{as}(Si)CH_3$
2955 _m	2955 _m	2954 _{sh,m}				$\nu_{as}CH_3$ (BO/CTAB)
			2934 _w	2933 _w	2935 _w	$\nu_{as}CH_2$ (APTMS)
2925 _m	2925 _m	2926 _m				$\nu_{as}CH_2$ (BO/CTAB)
			2912 _w	2913 _w	2912 _w	$\nu_s(Si)CH_3$
			2889 _w	2886 _w	2885 _w	ν_sCH_2 (APTMS)
			2868 _{sh,w}	2867 _w	2869 _{sh,w}	$\nu_s(Si)CH_2$ (APTMS)
2853 _m	2853 _m	2853 _m				ν_sCH_3 (BO/CTAB)
		1786/1765 _{vw}			1786/1765 _{vw}	$\nu C=O$ (BPO)
1717/1700 _{vw}	1724/1705 _{vw}		1737 _{vw}	1740/1727 _{vw}		$\nu C=O$ (BO)
		1707/1700 _w				$\nu C=O_{H-bonded}$ (BPO)
		1621 _{vw}				$\nu C=C$ (BPO)
1606 _{sh,vw}	1623/1607 _{vw}					$\nu C=C$ (BO)
		1595 _{vw}				$\nu C=C$ (BPO)
						$\nu C=C$ (BO)
			1577 _w	1579 _w	1582 _w	δNH_2 (APTMS)
1559 _w	1559 _w					$\nu C=C$ (BO)
		1543 _w				$\nu C=C$ (BPO)
1490 _{vw}	1490 _{vw}	1490 _{vw}				$\delta_{as}CH_3$ (CTAB)
			1486 _{vw}	1484 _{vw}	1488 _{vw}	δNH_2 (APTMS)
1478 _{vw}	1478 _{vw}	1478 _{vw}				$\delta_{as}CH_3$ (CTAB)
1468 _{vw}	1468 _{vw}	1468 _{vw}				$\delta_{as}CH_3$ (BO/CTAB)
		1451 _{vw}			1449 _{vw}	$\nu C=C$ (BPO)
1418 _{vw}	1418 _{vw}					$\delta_{as}CH_3$ (BO)
			1411 _{vw}	1411 _{vw}	1410 _{vw}	$\delta_{as}(Si)CH_3$
		1388 _m				$\delta C-H$ (BPO)
			1388 _{vw}	1388 _{vw}	1389 _{vw}	δ_sCH_3 (APTMS)
1380 _{vw}	1377 _{vw}					δ_sCH_3 (BO)
			1271 _s	1271 _s	1271 _s	$\delta_s(Si)CH_3$
1227 _{sh,vs}	1227 _{sh,vs}	$\approx 1230_{sh,vs}$	1126 _{vs}	1126 _{vs}	1124 _{vs}	$\nu_{as}Si-O-Si$
		1223/1173 _w				$\nu C-O$ (BPO)
1089 _{vs}	1082 _{vs}	1085 _{vs}	1038 _{vs}	1038 _{vs}	1035 _{vs}	$\nu_{as}Si-O-Si$
968 _m	966 _m	969 _m	938 _m	938 _m	938 _m	$\nu Si-OH$
			850 _{sh,w}	850 _{sh,w}	850 _{sh,w}	$\nu Si-C$
800 _m	802 _m	801 _m				$\nu_sSi-O-Si$
			780 _{vs}	780 _{vs}	779 _{vs}	$\nu_sSi-O-Si/\rho(Si)CH_3$
		716 _m				$\gamma(\text{ring})_{out-of-plane}$ (BPO)
550 _w	557 _w	561 _w	550 _{vw}	555 _{vw}	560 _{vw}	(SiO_4) rings
458 _s	458 _s	462 _s	442 _m	442 _m	$\approx 430_{sh,m}$	$\delta Si-O-Si$

[a] Values correspond to the band maximum.

samples is suggested by the bands at 1490, 1478, and 1468 cm^{-1} , assigned to CH_3 and CH_2 deformation modes. The surfactant bands contribute to the C–H stretching region as well and, for BO doped microcapsules, they may overlap with the dopant's bands. The above discussion was taken into account in the proposed band assignments summarized in Table 2.

Regarding the microcapsules' shells, the completely different structures of the silica and organosilica shells produced by each method were interpreted taking into account the fact that the elementary SiO_4 units are arranged mostly in four and six member siloxane rings, $(\text{SiO})_4$ and $(\text{SiO})_6$, and that the corresponding bands will be split into a pair of optical components (longitudinal and transverse), resulting from long range Coulomb interactions.^[17] To quantify the relative proportions of these components, the spectroscopic region containing the main silica band (1350–1000 cm^{-1}) was deconvoluted into a sum of Gaussian bands, by a nonlinear least-squares fitting method. The main results are summarized in Table 3.

Table 3. Band deconvolution results for microcapsule doped samples MEF8, MEF10, MME6, and MME7, between 1350 and 1000 cm^{-1} . Longitudinal (LO_x) and transverse optical (TO_x) component of $(\text{SiO})_x$ rings.				
Sample	Assignment	IR band [cm^{-1}] ^[a]	Area [%]	$(\text{SiO})_6$ [%]
MEF8	LO_6	1221	7.8	21.2
	LO_4	1148	52.7	
	TO_4	1086	24.2	
	TO_6	1050	12.9	
MEF10	LO_6	1226	7.0	19.0
	LO_4	1152	49.2	
	TO_4	1081	30.4	
	TO_6	1045	11.6	
MME6	LO_6	1131	41.6	89.5
	LO_4	1094	4.5	
	TO_4	1073	6.0	
	TO_6	1035	47.9	
MME7	LO_6	1127	46.2	92.9
	LO_4	1092	2.2	
	TO_4	1072	4.9	
	TO_6	1035	46.8	
MMB4	LO_6	1125	46.3	95.1
	LO_4	1091	1.8	
	TO_4	1073	3.1	
	TO_6	1033	48.8	

[a] Values correspond to the band center.

The fitted components confirm that the inorganic microcapsules (MEF8 and MEF10) have very similar structures: the predominant siloxane rings are $(\text{SiO})_4$ ($\approx 80\%$) and the LO-TO splitting values are not sensitive to ageing, thus showing that the structure of these microparticles is stable, at least for a period of six months. The same stability with ageing is observed for the organosilica microcapsules MME6, MME7, and MMB4, although the silica structure is very different: it is mostly composed of $(\text{SiO})_6$ siloxane rings ($\approx 90\%$), and with

much lower LO-TO splitting values. These are certainly much more porous materials, as expected from the low functionality of the selected precursors.^[18] Although the sol-gel silica structures usually have a "living" nature, these microparticles proved to be very stable. Another expected consequence of ageing is the evaporation of the encapsulated volatile dopant molecules through the microparticle's shell. Indeed, such evaporation was clearly observed for both the organic MM and the inorganic ME capsule samples.

In conclusion, DRIFT spectroscopy was applied to study a series of silica-based microparticles doped with polymerization catalyst benzoyl peroxide and perfumed bergamot oil. Core/shell silica- and organosilica-based microparticles were prepared from O/W emulsions, resulting in widely different compartmentalization of the active compounds inside the resulting core/shell microcapsules. The first relevant conclusion is that neither BPO nor BO degrades upon encapsulation in these microcapsules. In the case of bergamot oil, a more efficient entrapment occurs in silica microcapsules obtained from ammonia-catalyzed condensation of TEOS assisted by surfactant CTAB. Evaporation of the entrapped fragrance chemicals in the core of the capsules is slow, as shown by the slight change in the fingerprint signals of the most abundant terpenes comprising the essential oil in the microparticles aged for six months. When peroxide BPO is entrapped, on the other hand, the best encapsulation requires a methyl-modified organosilica shell obtained from ammonia-catalyzed condensation of TEOS assisted by surfactant CTAB.

Contrary to expectations, entrapment in fully methyl-modified microparticles obtained from polycondensation of MTMOS catalyzed by amino-propyl trimethoxysilane is poor in both cases (either for BO or BPO), and is most likely due to the employment of the ethanol/water solvent system in the polycondensation, which favors migration and loss of dopant molecules from the liquid core of the core/shell microcapsules. The method, therefore, is not suitable for practical microencapsulation of these functional molecules.

These results are of relevance to a number of forthcoming applications of sol-gel microcapsules. For example, in general, encapsulation of aroma chemicals in micron-sized particles that contain an active agent surrounded by an inert shell, affording controlled release and delivery, stabilizes the core material and thus allows the employment during processing, storage, and usage of unstable biodegradable fragrance molecules.^[11] We are continuing to investigate these materials in light of catalytic and cosmetic applications.

Experimental Section

Several silica (from tetraethoxysilane, TEOS) and methyl-modified silica (from methyltrimethoxysilane, MTMOS) microparticles doped with BO or BPO were prepared by the sol-gel process, at room temperature, according to the O/W polycondensation method, catalyzed by ammonia (with cetyltrimethylammonium bromide (CTAB) as the surfactant) or by 3-aminopropyltrimethoxysilane (APTMS). All chemicals were purchased from Aldrich and were used without

further purification. The samples' compositions and labels are summarized in Table 1 and the preparation details are described below.

Samples MEF8 and MEF10

A solution of deionized water (125 mL), ethanol (75 mL), CTAB (1.5 mL, 25 wt%), and aqueous ammonia (2.5 mL, 25 wt%), kept under stirring (700 rpm, magnetic stirrer), was mixed with a solution of BO (2 mL) in TEOS (10.2 mL). Stirring was then set at 500 rpm and the resulting mixture left under agitation for 24 h, after which time a pale yellow precipitate was filtered through a filter paper (Whatman grade no. 1, 1001–185), washed with water, and left to dry at RT for 24 h. Sample **MEF10** was prepared six months after sample **MEF8** by using the same reaction protocol.

Sample MEB9

A solution of deionized water (125 mL), ethanol (75 mL), CTAB (1.5 mL, 25 wt%), and aqueous ammonia (2.5 mL, 25 wt%), kept under stirring (700 rpm, magnetic stirrer), was mixed with a solution of TEOS (8.2 mL), MTMOS (1.2 mL), and BPO (Luperox 70: BPO 70 wt% in water, 666.7 mg) dissolved in toluene (3.7 mL). Stirring was then set at 500 rpm and the resulting mixture left under agitation for 24 h, after which time the white precipitate was filtered, washed with water, and dried at 40 °C for three days.

Samples MME6 and MME7

A solution of deionized water (150 mL) and 3-aminopropyl trimethoxysilane (APTMS, 3 mL) was mixed under stirring (magnetic stirrer, 1000 rpm) with a solution of methyltrimethoxysilane (MTMOS, 9 mL) and BO (3 mL). The resulting mixture was left under agitation for 24 h, after which time a pale yellow precipitate was filtered, washed extensively with deionized water, and left to dry for 24 h at RT. Sample **MME7** was prepared six months after sample **MME6** by using the same reaction protocol.

Sample MMB4

A solution of deionized water (150 mL) and 3-aminopropyl trimethoxysilane (APTMS, 3 mL) was mixed under stirring (1000 rpm, magnetic stirrer) with a solution of methyltrimethoxysilane (MTMOS, 9 mL) and BPO (Luperox 0: BPO 70 wt% in water, 300 mg). The resulting mixture was left under agitation for 24 h, after which time a pale yellow precipitate was filtered, washed extensively with deionized water, and dried in an oven at 50 °C for three days.

Acknowledgements

This Communication is dedicated with affection to University of Palermo's Professor Roberto Zingales, for all the years devoted to the education of young chemists. A.F. gratefully acknowledges Fundação para a Ciência e a Tecnologia (FCT, Portugal) for a post-doctoral grant SFRH/BPD/66379/2009. We thank Capua 1990 Srl (Campo Calabro, Italy) for a gift of crude bergamot oil. M.S. thanks Greenseal Chemicals (Ghent, Belgium) for continuous support throughout her doctorate.

Keywords: core/shell structures • microencapsulation • organosilica • self-assembly • sol-gel processes

- [1] M. Pagliaro, M. Sciortino, R. Ciriminna, G. Alonzo, A. De Schrijver, *Chem. Rev.* **2011**, *111*, 765–789.
- [2] C. J. A. Barbé, J. Bartlett, L. Kong, K. Finnie, H. Q. Lin, M. Larkin, S. Calleja, A. Bush, G. Calleja, *Adv. Mater.* **2004**, *16*, 1959–1966.
- [3] N. Lapidot, S. Magdassi, D. Avnir, C. Rottman, O. Gans, A. Seri-Levy, WO 2003/80823.
- [4] J. Borges Lobo, PhD Thesis, Technical University of Lisboa, **2008**.
- [5] H. Liu, C. Z. Chuai, M. Iqbal, H. S. Wang, B. B. Kalsoom, M. Khattak, M. Q. Khattak, *J. Appl. Polym. Sci.* **2011**, *122*, 973–980.
- [6] G. M. Keating, *American Journal of Clinical Dermatology* **2011**, *12*, 407–420.
- [7] J. Emer, H. Waldorf, D. Berson, *Seminars in Cutaneous Medicine and Surgery* **2011**, *30*, 148–155.
- [8] http://en.wikipedia.org/wiki/Bergamot_orange.
- [9] H. Tapanee, *Nat. Prod. Commun.* **2011**, *6*, 1199–1204.
- [10] N. Jeffries, *Beauty Game Changers, Household & Personal Products Industry* **2009**, *46*, 42.
- [11] J. J. G. van Soest in *Encapsulation of Fragrances and Flavours: a Way to Control Odours and Aroma in Consumer Products, Chemistry, Bioprocessing and Sustainability*, (Ed.: R. G. Berger), Springer, Berlin, **2007**.
- [12] M. Sciortino, M. Pagliaro, R. Ciriminna, G. Alonzo, *Silicon* **2011**, *3*, 77–83.
- [13] C. Rottman, G. Grader, Y. De Hazan, S. Melchior, D. Avnir, *J. Am. Chem. Soc.* **1999**, *121*, 8533–8543.
- [14] B. Fei, H. Lu, R. H. Wang, J. H. Xin, *Chem. Lett.* **2006**, *35*, 622–623.
- [15] F. Partal Uren~a, J. R. A. Moreno, J. J. L. Gonzalez, *J. Phys. Chem. A* **2008**, *112*, 7887–7893.
- [16] V. Vacque, B. Sombret, J. P. Huvenne, P. Legrand, S. Such, *Spectrochim. Acta Part A* **1997**, *53*, 55–66.
- [17] A. Fidalgo, L. M. Ilharco, *Chem. Eur. J.* **2004**, *10*, 392–398.
- [18] A. Fidalgo, R. Ciriminna, L. M. Ilharco, M. Pagliaro, *Chem. Mater.* **2005**, *17*, 6686–6694.

Received: April 4, 2012

Published online on May 21, 2012